Thermal behavior, FT-IR spectroscopy and water durability of Li₂O–PbO–ZnO–P₂O₅ glasses

M. Abid [1,3,*], M. Belfaquir [2], M. Hafid [3] and M. Taibi [4]

[1] *Regional Center for Education and Training Trades, Rabat-Salé-Kenitra Region, Laboratoire de Physique-Chimie, Morocco,*
[2] *Ibn Tofail University, FSK, Laboratoire des Matériaux, Electrochimie et Environnement, B. P., 133, 14000 Kénitra, Morocco,*
[3] *Ibn Tofail University, FSK, Laboratoire de Physico-Chimie des Matériaux et Environnement, B.P., 133, 14000 Kénitra, Morocco,*
[4] *Mohammed V University, ENS Takaddoum, Laboratoire de Physico-Chimie des Matériaux Inorganiques et Organiques(LPCMIO), B.P. 5118, Rabat 10000, Morocco.*

Abstract

Lithium–lead–zinc phosphate glasses having a composition $(35-y)Li_2O–yPbO–15ZnO–50P_2O_5$ ($0 \leq y \leq 35$ mol%) were prepared by using the melt–quench technique. Their structures have been characterized by infrared spectroscopy. The substitution of 15 mol% ZnO and 35 mol% PbO for 50 mol% Li_2O in the binary $50Li_2O–50P_2O_5$ glass decreases the molar volume ($\Delta V_m = 2.62$ cm³/mol) and increases further the glass transition temperature ($\Delta T_g = 70$ °C). FTIR spectra reveal the formation of P–O–Pb and P–O–Zn bonds in these glasses and show that metaphosphate network is not affected when PbO content increases. Thus, PbO is assumed to play an intermediate role in a way that Pb^{2+} cation tends to break P–O–P bonds forming PbO_4 units with covalent Pb–O bonds. The predominant structural units in all these glasses are metaphosphate $(P_2O_6)^{2-}$ groups. Moreover, systematic variations of the glass transition temperature, density, and molar volume observed are in agreement with these results. The durability of the studied glasses in the water is enhanced as PbO contents increases.

1. Introduction

Phosphate glasses are more advantageous than conventional silicate and borate glasses because they generally offer some unique physical properties such as high thermal expansion coefficients, low melting temperature, low softening temperature, high electrical conductivity, high ultra-violet transmission and optical characteristics [1-8]. Phosphate glasses have also emerged as a promising group of glasses for optical amplifiers, fibers, laser, etc. [9]. However, the poor chemical durability, high hygroscopic and volatile nature of phosphate glasses have restricted their use for replacing the conventional glasses for a developed range of technological applications [10,11]. The structural investigations of phosphorous in former P_2O_5 basic glass have shown that P^{5+} ions are tetrahedrally co-ordinated by oxygen atoms and tetrahedral units are corner bonded in a random configuration [12]. The structure of phosphate glasses is based on the distribution of Q^i nomenclature, where "i" (i = 0, 1, 2 or 3) represents the number of bridging oxygens (BO) per PO_4 tetrahedron in the vitreous network. Depending on the [O]/[P] ratio defined by a glass composition, the phosphate glasses can be described by different structures: cross-linked network of Q^3 tetrahedra (as for vitreous P_2O_5); polymer-like metaphosphate chains of Q^2 tetrahedra; 'invert' glasses based on small pyro (Q^1) and orthophosphate (Q^0) species [5]. The physical properties and chemical durability of phosphate glasses are found to be improved by introducing of one or more of multivalent oxides into P_2O_5 glass network such as PbO, ZnO, Al_2O_3, MoO_3, WO_3, TiO_2 etc. which extends their applications [13-17] even in the burial of radioactive wastes. Thus, the phosphate glasses with addition of heavy metal oxide have been found to be used in broad range of applications, such as photonic, bone regeneration and hermetic sealing technology.

In the previous works, the oxide glasses containing transition metal ions are of great interest because of their semiconducting properties. It has been reported that the addition of zinc oxide ZnO can improve resistance of a glass to aqueous attack because Zn^{2+} ion acts as an ionic cross linker between different phosphate anions, inhibiting hydration reaction [18-20]. Zinc oxide ZnO acts a glass modifier, where Zn^{2+} occupies interstitial sites in glass network [21].

Among various modifier oxides that play the role of glass modifiers in P_2O_5 glass network, the lead-oxide (PbO) is considered as unique since PbO is known to play a dual structural role as well as a modifier and a former network. Recently, further studies have been made on lead phosphate glasses using Raman, FTIR, NMR, X-ray diffraction techniques [22–29]. These studies revealed that lead oxide PbO takes the role of both glass former and glass modifier. As a glass former, PbO enters the network with PbO_4 structural units by sharing the corners of phosphate network which in turn form P–O–Pb linkages. When PbO acts as a network modifier, Pb^{2+} ion becomes of octahedral coordination like any other conventional alkali oxide modifier. Studies of, a various properties of ternary $PbO–ZnO–P_2O_5$ glasses were carried out [30–35]. The main attention was given to the glasses with the molar content of P_2O_5 is around 50%. The lead zinc phosphate glasses are known as materials considered for nuclear wastes storage [36], and owing to their low glass-transition temperature and suitable high thermal expansion coefficients, they are also interesting for some sealing applications [37]. On the other hand, lithium ion conducting glasses have enormous potential for uses in electrochemical devices, such as solid-state batteries, sensors, electrochemical capacitors, electro-chromic displays and analog memory devices [38]. The specific applications of the quaternary $Li_2O–PbO–ZnO–P_2O_5$ glasses make the knowledge of their structure-properties relationships challenging. However, only few studies have been devoted to the characterization of their structure [39-41]. In the present work, the structure of glasses with the general composition $(35–y)Li_2O–yPbO–15ZnO–50P_2O_5$ (0≤y≤35 mol%) is investigated using IR spectroscopy in order to elucidate the structure of the glass as a function of composition. Other properties, such as density, molar volume, glass transition temperature and water durability, are investigated and correlated with the structure changes.

2. Material and Methods

2.1. Preparation of glasses

Glasses of the target composition were prepared by mixing the appropriate amounts of lithium carbonate Li_2CO_3, lead oxide PbO, zinc oxide ZnO and diammonium hydrogen phosphate $(NH_4)_2HPO_4$ according to the reaction scheme:

$xLi_2CO_3 + yPbO + zZnO + 2t(NH_4)_2HPO_4$ ➔ $[xLi_2O, yPbO, zZnO, tP_2O_5] + 4tNH_3 + 3tH_2O + xCO_2$

Where x, y, z and t are molar percentage of Li_2O, PbO, ZnO and P_2O_5 respectively; x=(35–y), z=15, t=50, (0≤y≤35 mol%)

Mixtures of the starting materials were firstly ground in an agate mortar and preheated in alumina crucible at 120°C overnight. They were then annealed at the temperatures varying between 300 and 400°C for 12 h to remove NH_3, H_2O, and CO_2. The temperature was then progressively increased to 1050°C and held constant at this value for 15min. The batch was finally quenched to room temperature under air atmosphere to produce vitreous samples.

2.2. X-ray diffraction study

X-ray diffractograms of the powdered samples were recorded at room temperature using a Siemens D5000 diffractometer with Cu_K radiation (λ = 1,5418 Å) in the 2θ ranges of 10 °- 60 ° at a scanning rate of 2 ° per minute. The XRD analysis was used to confirm the amorphous nature of the glasses.

2.3. Thermal study

Differential scanning calorimetry of powder samples was made at a heating rate of 10 K.min^{-1} using the DSC-SETRAM type apparatus 121 to determine the glass transition temperature (T_g); the estimated error is ±5 °C.

2.4. Density measurements

Density measurements were carried out at room temperature, using Archimedes method with xylène as the immersion fluid. The relative error in these measurements was about ±0.03 g.cm^{-3}.

2.5. Infrared spectroscopy study

The Fourier transform infrared (FTIR) spectroscopy measurements were made on glass powders dispersed in KBr pellets (3 wt.%). The infrared spectra of the powder glass samples were recorded at room temperature in the range between 400 –1400 cm^{-1} using a FTIR Perkin-Elmer spectrometer.

2.6. Water durability

The water durability behavior of the bulk glasses was followed in static regime and evaluated from the weight of samples immersed in deionized water for 28 days. The samples were polished to 600 grit finished with SiC paper, cleaned with acetone and suspended in glass flasks containing deionized water at 25±3 °C. The glass surface area to solution volume ratio (S/V) was 0.02 cm^{-1}. The weight loss (Δw) of the samples was measured at various time points (1, 7, 14, 21 and 28 days). The samples were measured before and after different immersion times, by using an analytic balance of sensitivity 0.1mg. The weight loss (Δw) was obtained from the relation: $\Delta w = w_0 - w$, where w_0 and w is original and remain weight (g) of sample glass, respectively. The dissolution rate (DR) was calculated as: $DR = \Delta w / (Axt)$ where Δw is the weight loss (g), A is the sample area (cm^2) before the dissolution test and t is the dissolution time (min).

3. Results and discussion

The obtained results concerning nominal compositions, density, molar volume, glass transition temperature and dissolution rates DR for all studied samples are listed in Table 1.

Table 1: Composition, density ρ, molar volume V_m, glass transition temperature T_g and dissolution rates DR in 28 days of LiPbZnP glasses

y (mol%)	Glass compositions (mol%)	ρ (g/cm^3)	V_m (cm^3/mol)	T_g (°C)	DR (g/cm^2/min)
y=0	$35Li_2O–15ZnO–50P_2O_5$	2.51	37.30	333	1.64×10^{-6}
y=5	$30Li_2O–5PbO–15ZnO–50P_2O_5$	2.78	37.16	334	8.02×10^{-7}
y=15	$20Li_2O–15PbO–15ZnO–50P_2O_5$	3.35	36.60	336	2.52×10^{-7}
y=25	$10Li_2O–25PbO–15ZnO–50P_2O_5$	4.00	35.49	344	7.23×10^{-8}
y=35	$35PbO–15ZnO–50P_2O_5$	4.62	34.91	373	2.08×10^{-8}

3.1. X-ray diffraction

As shown in figure 1, the X-ray diffraction patterns of typical glass sample, with nominal composition of $20Li_2O–15PbO–15ZnO–50P_2O_5$ confirms their amorphous nature, since there is no sharp peak observed in the diffraction pattern.
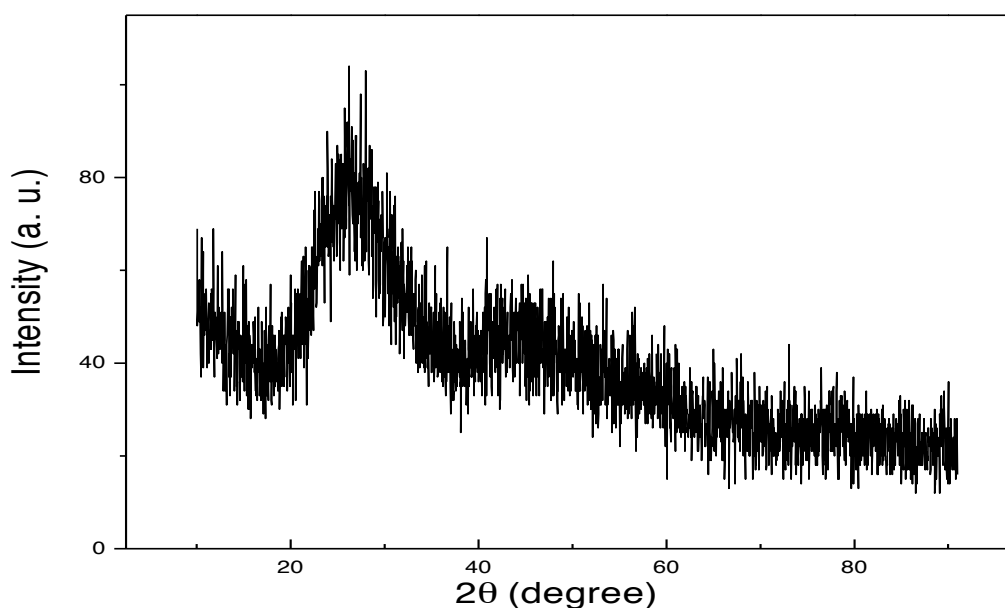

Figure 1: X-ray diffraction patterns for typical glass $20Li_2O–15PbO–15ZnO–50P_2O_5$

3.2. Density and molar volume

The molar volume of the glass, V_m was calculated from the molecular weight, M and density ρ ($V_m = M/\rho$). The molecular weight, M was calculated using the relation:

$M(Glass) = (35-y) \times M(Li_2O) + y \times M(PbO) + 15 \times M(ZnO) + 50 \times M(P_2O_5)$.

where (35–z), y, 15 and 50 are the mole percent of Li_2O, PbO, ZnO and P_2O_5 respectively: $M(Li_2O)$, $M(PbO)$, $M(ZnO)$ and $M(P_2O_5)$ are their respective molecular weights.

Density is a useful parameter to measure when investigating changes in the structure of glasses, as it is affected by structural softening/compactness, changes in geometrical configuration, coordination number, cross-link density and the dimensions of interstitial spaces in the structure. The values of density and molar volume of each sample are listed in Table 1 and are graphically represented in figure 2.

Density values of $35Li_2O-15ZnO-50P_2O_5$ (y=0) glasses (table 1) and $50Li_2O-50P_2O_5$ are 2.51 g/cm^3 and 2.29 g/cm^3 [41], respectively. Substitution of Li_2O by ZnO increases largely the density. As shown in Fig. 2, the density increases with increasing PbO content in LiPbZnP metaphosphate glasses, density increases from 2.51g/cm^3 (%PbO=0) to 4.62 g/cm^3 (%PbO=35). In general, the increase in the density can be related to either the constitutions of the glass or to the structural variation in the type of phosphate structural units. At the first sight, the increase in the density of the studied glasses can be related to the replacement of oxide Li_2O have lower molecular weight (29,88 g. mol^{-1}) by an oxide which has a greater molecular weight like ZnO (81,3794 g.mol^{-1}) or PbO (223,1994 g.mol^{-1}).
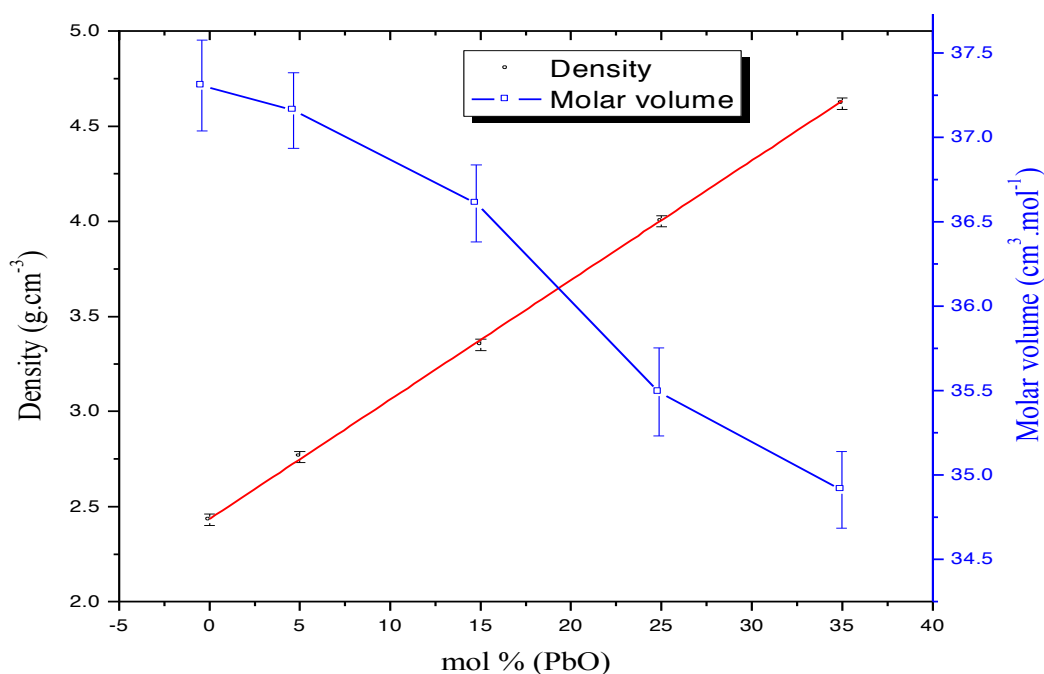

Figure 2: Composition dependence of density and molar volume of LiPbZnP glasses

The substitution of 15 mol% ZnO for 15 mol% Li_2O in zinc free lithium metaphosphate glass results in a decrease in molar volume from 37.53 cm^3. mol^{-1} for $50Li_2O-50P_2O_5$ glass [41] to 37.30 cm^3. mol^{-1} for $35Li_2O-15ZnO-50P_2O_5$ glass. When PbO is substituted for Li_2O in LiPbZnP phosphate glasses, there is a non-linear decrease of molar volume V_m up to 34.91 cm^3. mol^{-1} (y=35) (Figure 2), while the density varies quite linearly. This suggests that substitution of Li_2O by PbO, in LiPbZnP phosphate glasses, is far from ideal and it will change the glass structure (shorten the phosphate chain length) and make it more compact. The non-linear decrease of molar volume V_m can be explained by the formation of Pb–O bonds [30, 41, 47- 48], with a covalent nature more than that of Li–O bonds, which reticule the phosphate network and lead to the close structure of the glasses. Similarly, such a point of view was also used to interpret the formation of covalent Pb–O bonds in ternary lead lithium phosphate glasses [41].

3.3. Glass transition temperature

In figure 3, a typical DSC curve of chosen glass composition of $35Li_2O-15ZnO-50P_2O_5$ (y=0) is represented. Similar curves have been recorded for all other samples given in Table 1. From the DSC curve, we can obtain the glass transition temperature T_g for each composition (Table 1).
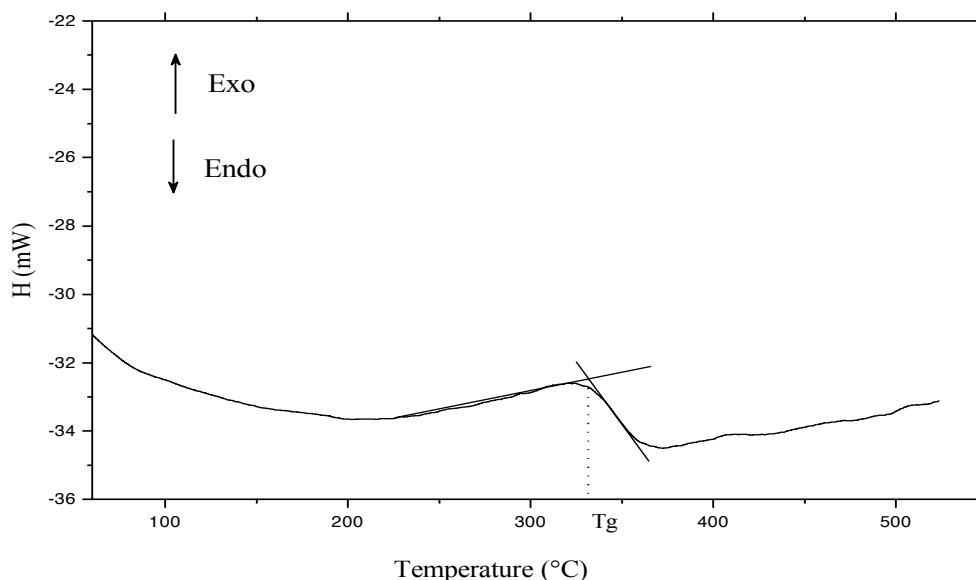
Figure 3: DSC curve of glass with composition of $35Li_2O–15ZnO–50P_2O_5$

DSC measurements give the variation of T_g from 303°C for binary lithium phosphate glass of composition $50Li_2O–50P_2O_5$ [41] to 333°C for lithium zinc metaphosphate glass of composition $35Li_2O–15ZnO–50P_2O_5$ (y=0) (Table 1). The substitution of 15 mol% ZnO for 15 mol% Li_2O leads to the significant increase of T_g in the glass (30°C) and shows that the structure is strongly modified.

The glass transition temperature T_g of the LiPbZnP phosphate glasses increases also but slowly for (0<y≤25) (11°C) and rapidly for 25<y≤35 (29°C) as PbO replaces Li_2O with a fixed ZnO and P_2O_5 contents of 15 and 50 mol% respectively (Figure 4).

We suppose that in these glasses, when zinc (Zn^{2+}) and lead (Pb^{2+}) cations substitute for lithium ($2Li^+$) ions (in $50Li_2O–50P_2O_5$ glass for Zn^{2+}, and in $35Li_2O–15ZnO–50P_2O_5$ glass for Pb^{2+}), $–P–O_\delta^-...Zn_\delta^+$ and $–P–O_\delta^-...Pb_\delta^+$ bonds are formed with a strong covalent Zn–O and Pb–O bonds than Li–O (the Zn and Pb electronegativities being larger than that of Li). This behavior means that the transition temperature increases in PbO-rich phosphate glasses [49]. We assume that in this case lead and Zinc can be incorporated into the network resulting in the formation of P–O–Pb and P–O–Zn linkages respectively.
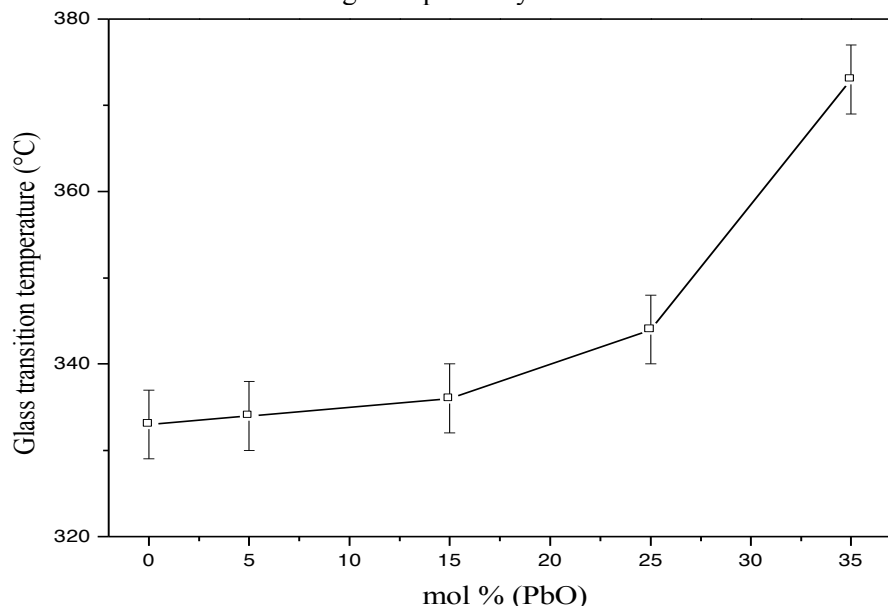

Figure 4: Composition dependence of glass transition temperature for LiPbZnP glasses

3.4. FT-IR spectra analysis

FTIR spectra of LiPbZnP metaphosphate glasses with various contents of lead oxide (PbO) ranging from 0 to 35 mol%, in the frequency range between 400 and 1400 cm^{-1}, are shown in Figure 5.
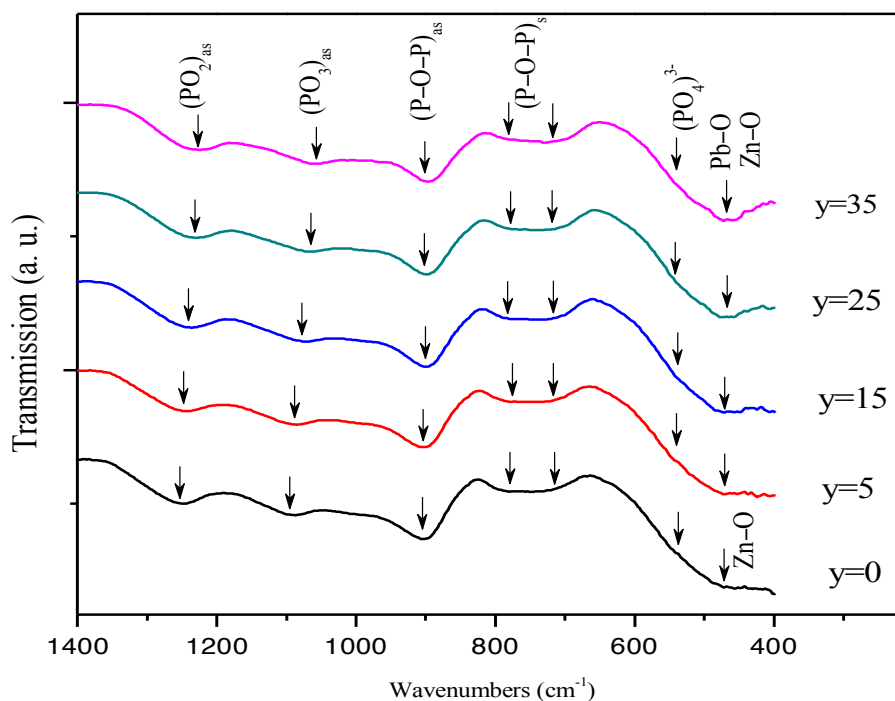
Figure 5: Infrared spectra of LiPbZnP glasses

3.4.1. Lithium–Zinc–Metaphosphate glass (y=0)

The characteristic features of $35Li_2O-15ZnO-50P_2O_5$ glass (y=0) spectrum are the band at 1257 cm^{-1} attributed to the asymmetric stretching vibration band of the non-bridging oxygen atoms (NBO) bonded to phosphorus atoms PO_2 (Q^2 structural units) [22, 26, 41, 42]. The absorption band around 1095 cm^{-1} is assigned to asymmetric stretching of PO_3 groups characteristic of Q^1 structural units (chain-end groups) [20, 22, 43]. The band at 901 cm^{-1} is assigned to asymmetric stretching of P–O–P bridges [23, 27, 43-46], whereas the absorption bands at 776 and 714 cm^{-1} are due to symmetric stretching of P–O–P bridges [45]. However, the glass is found to exhibit two bands in the frequency range 776–714 cm^{-1} which are ascribed to the presence of two P–O–P units in metaphosphate chain based on ($P_2O_6^{2-}$) cyclic groups as shown in Figure 6 [50, 51]. The band around 534 cm^{-1} is due to deformation modes of P–O$^-$ bonds (υPO_4^{3-}) [31, 46], whilst a new absorption weak band at about 470 cm^{-1}. It suggests that the bands characteristics of Zn–O (or Pb–O) vibrations remain in the region below 600 cm^{-1}, while bands above 600 cm^{-1} are likely caused by vibrations of phosphate network. In zinc silicate glasses, the Zn–O tetrahedral bond is in the range of 600–400 cm^{-1}, while the Zn–O octahedral bonds lies at 300-100 cm^{-1}[52]. This postulation is further supported by various authors [44, 53], and in our case, we presumed the band at about 470 cm^{-1} is assigned to the vibration of Zn–O in ZnO_4 groups [30, 39, 54].
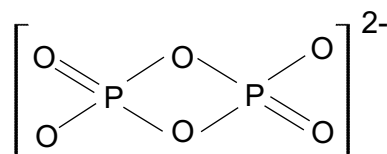

Figure 6: Metaphosphate (P_2O_6)$^{2-}$ contains two P–O–P units

3.4.2. Lithium–Lead–Zinc–Metaphosphate glasses (5≤y≤35)

The IR spectra of all the glasses of compositions LiPbZnP are typical to the spectrum of lithium–zinc–metaphosphate glass of composition $35Li_2O-15ZnO-50P_2O_5$ (Figure 5). The infrared spectra for all these glasses clearly show that the structure of the phosphate chains is not affected by the substitution of Pb^{2+} for Li^+ in the glass, indicating that the fraction of bridging oxygens (P–O–P) is unaffected by glass compositions, which agrees with the atomic oxygen/phosphorus ratio of (O/P) equal to 3 in batch composition. The figure 7 show that the band frequencies of PO_2 symmetric stretching mode shifts to lower frequencies as PbO content increases from 1257 cm^{-1} for $35Li_2O-15ZnO-50P_2O_5$ glass (y=0) to 1224 cm^{-1} for $35PbO-15ZnO-50P_2O_5$ glass (y=35). The variation of asymmetric stretching modes of PO_2 units can be attributed to: (1) the larger field strength F_{M-O} of Pb^{2+} (=31 nm^{-2}) > Li^+ (=23 nm^{-2}), (2) metal atomic weight being larger in the order M(Pb)=207,2 u > M(Li)=6,941 u, that affects the metal to nonbridging oxygen bond along phosphate chains.

This behaviour agrees with the proposed model of Rouse et al [55] in alkali metal metaphosphate glasses. The model suggests that the frequency of symmetric and asymmetric of PO_2 stretch will vary systematically with substituted cation (cation mass, M_c), force constant in the alkali–nonbridging oxygen bond (F_{m-O}) and O–P–O bond angle ($v(PO_2)$).
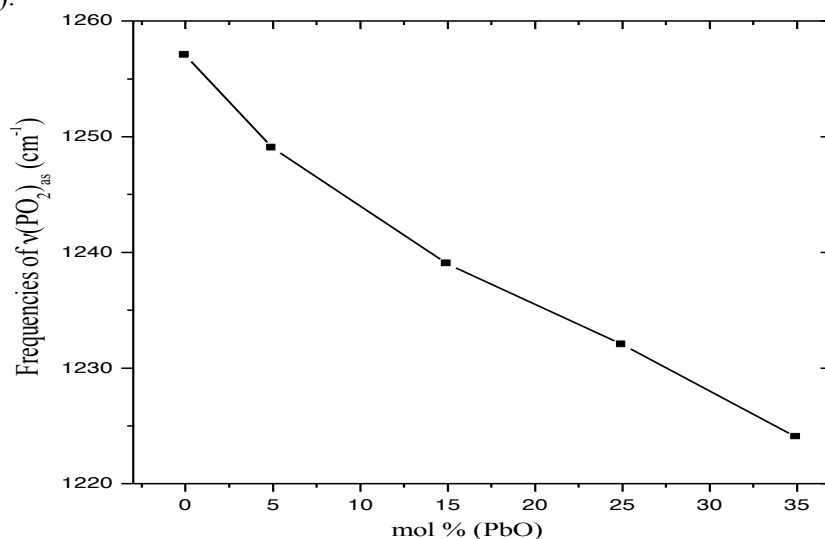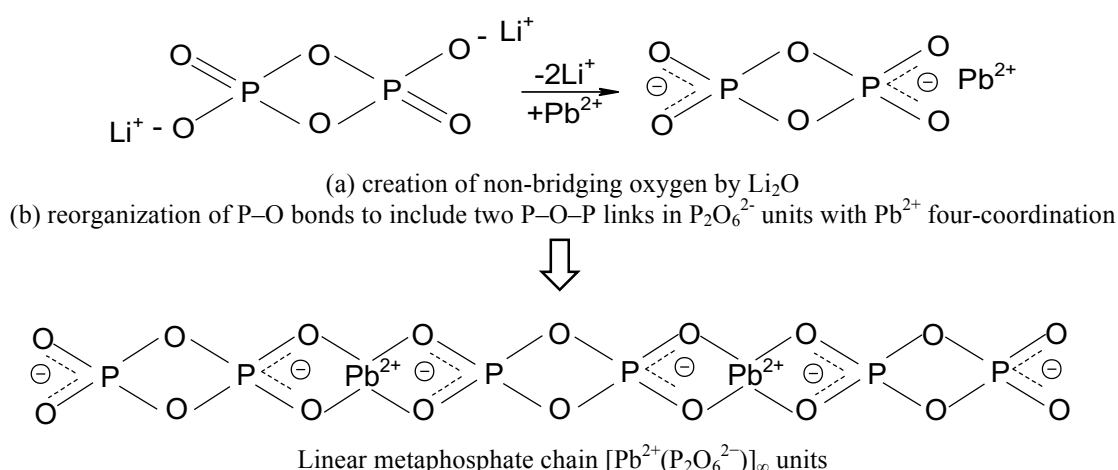

Figure 7: Frequencies variations of $v(PO_2)_{as}$ modes vs PbO content in LiPbZnP glasses

Bands frequencies of P–O–P symmetric stretching modes shift slightly to higher frequency as the PbO content increases from 776/714 cm^{-1} for $35Li_2O$–$15ZnO$–$50P_2O_5$ (y=0) to 781/717 for $35PbO$–$15ZnO$–$50P_2O_5$ glass (y=35). The shift bands frequencies can be explained by the increase in covalent character of P–O–P bonds and indicates that the P–O–P bonds are strengthened as PbO is substituted for Li_2O. The low frequency band near 530 cm^{-1} (shoulder), which is attributed to deformation modes of P–O$^-$ bonds (vPO_4^{3-}), is also present in all these glasses. Moreover, a narrow low frequency band appears at about 470 cm^{-1} probably due to Pb–O stretching in PbO_4 units and Zn–O stretching can clearly be observed in the spectra of all the glasses. Similar to that observed in the IR spectra of phosphate glasses containing lead oxide [56–62]. Significant changes are observed in the intensity of the band at 470 cm^{-1} owing to the vibration of Pb–O linkages with increasing PbO content and became maximum in the spectrum of the glass $35PbO$–$15ZnO$–$50P_2O_5$ (y= 35). Thus, these results indicate that PbO is assumed to play an intermediate role. Li^+ cation is solely modifier ion while Pb^{2+} cation tends to break P–O–P bonds forming PbO_4 tetrahedral units connect to the phosphate tetrahedra PO_4 by P–O–Pb covalent bonding. The decrease in molar volume V_m and increase in T_g (Table 1) with increasing PbO content supports this deduction. The process of incorporation of PbO into the network may therefore be represented as:

(a) creation of non-bridging oxygen by Li_2O
(b) reorganization of P–O bonds to include two P–O–P links in $P_2O_6^{2-}$ units with Pb^{2+} four-coordination

Linear metaphosphate chain $[Pb^{2+}(P_2O_6^{2-})]_\infty$ units

3.4. Water durability
The water durability as determined by the sample weight loss per unit area ($\Delta w/A$) versus time in deionized water at 25 °C of LiPbZnP at various time points is shown in Figure 8. We can notice in this figure that water durability of these glasses is found to be sensitive to the glass composition. It can be seen clearly that the glasses whose PbO content is equal or more than 15 mol% have much better water durability (less weight loss). For example, in 28 days, weight loss decreases from 6,6 mg/cm^2 for free lead glass of composition ($35Li_2O$–

15ZnO–50P$_2$O$_5$) (y=0) to 0.84 mg/cm^2 for 35PbO–15ZnO–50P$_2$O$_5$ glass (y=35). This result indicates that the addition of lead to phosphate glasses will improve their chemical durability.
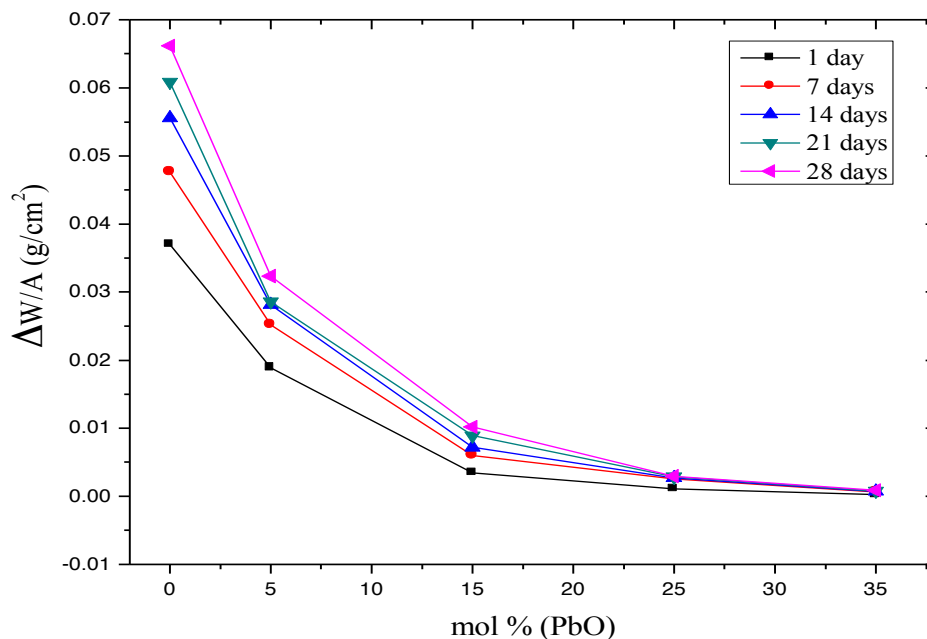

Figure 8: Weight loss per unit area of LiPbZnP glasses, as a function of the PbO content after immersion in distilled water at 25 °C for 1, 7, 14, 21 and 28 days.

The Figure 9 shows the effect of PbO concentration in the glass on the dissolution rates at different times of LiPbZnP metaphosphate glasses immersed in distilled water at 25°C. Obviously, the dissolution rate DR is higher for all the glasses in the beginning (first days) but decelerated with time.
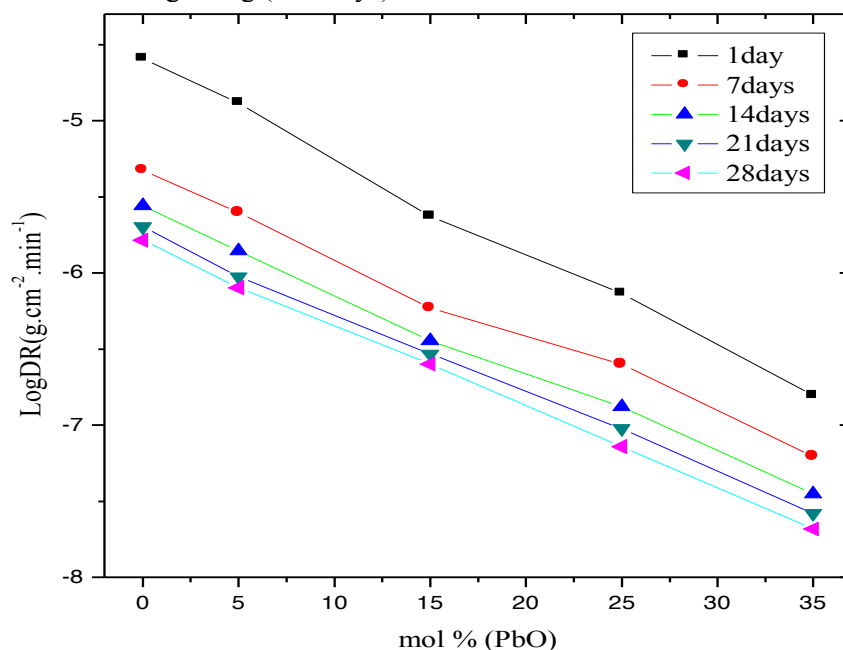

Figure 9: Dissolution rates (DR) of LiPbZnP glasses, as a function of the PbO content after immersion in distilled water at 25 °C for 1, 7, 14, 21 and 28 days.

It was also observed that the average DR is higher for free lead glass (35Li$_2$O–15ZnO–50P$_2$O$_5$) (y=0) than those observed for all other glasses. For example, the data obtained from DR in 28 days, showed that DR decreases from $1,64 \times 10^{-6}$ g.cm^{-2}.min^{-1}, for 35Li$_2$O–15ZnO–50P$_2$O$_5$ glass to $2,08 \times 10^{-8}$ g.cm^{-2}.min^{-1} for the 35PbO–15ZnO–50P$_2$O$_5$ glass (Table 1). This result indicates that the substitution of lithium oxide (Li$_2$O) with lead oxide (PbO) in metaphosphate glasses will improve their water durability. The best water durability of glasses rich lead oxide, may be attributed to the reticulation of the phosphate network by PbO$_4$ groups via Pb–O–P bonds which are more chemically durable than P–O–P and P–O$^-$..Li$^+$ bonds.

Several studies of the dissolution mechanism of phosphate glasses in aqueous solutions have been carried out [19, 63–65] and showed that phosphate glasses might dissolve by one of two mechanisms: hydrolysis or hydration reactions. The hydrolysis reaction of covalent P–O–P bonds would result in the ultimate cleavage of the phosphate network to produce orthophosphate. On the other hand, the hydration reaction occurs at modifier cations, disrupting ionic bonds between the phosphate chains. Therefore, the chemical durability of LiPbZnP metaphosphate glasses have been postulated to depend mostly on the ionic cross-links of Li^+, Zn^{2+} and Pb^{2+} cations between the phosphate chains.

Indeed, the structure of lithium zinc metaphosphate glass ($35Li_2O$-$15ZnO$-$50P_2O_5$) consists of a network of PO_4 tetrahedral units with two P–O–P bridges chain based on ($P_2O_6^{2-}$) groups as proposed by IR spectroscopy. Lithium oxide (Li_2O) and Zinc oxide (ZnO) in this glass convert the three-dimensional PO_4 network of phosphate glass into linear phosphate chains groups ($P_2O_6^{2-}$) with the cleavage of P–O–P linkages and creation of non-bridging oxygen (NBOs) atoms. The higher of PbO content, the higher chemical durability is, i.e; PbO improves the water resistance ability of phosphate glass. The metaphosphate glass ($35PbO–15ZnO–50P_2O_5$) occurs the lower values of DR and hence, good chemical durability. So, the improved water durability of the LiPbZnP glasses can be attributed to the replacement of the easily hydrolysed P–O–P and/or hydrated P–O…Li bonds by corrosion resistant P–O–Pb and/ or P–O–Zn bonds and also by reducing the non-bridging oxygen (NBOs) which results in a higher field strength, therefore, serves as a strong ionic cross-link between the non-bridging oxygens (NBOs) of two different phosphate chains. Thus, replacing lithium oxide by lead oxide, increases the number of P–O–Pb which will retard the entrance of H_2O molecules, and lead to decrease the dissolution rate of the phosphate glasses that increases the chemical durability. It has been found that cross-linking agents such as Al_2O_3, Fe_2O_3, Ag_2O, and PbO are effective additives to improve the chemical durability of phosphate glasses [64].

 Conclusions

Density, molar volume, thermal and Infrared spectroscopy studies have allowed us to follow the evolution of the glass structure of $(35-y)Li_2O–yPbO–15ZnO–50P_2O_5$ ($0{\leq}y{\leq}35$) glasses. The infrared spectra show that the structure of the phosphate chains is not affected by the substitution of Pb^{2+} for Li^+ in the glass metaphosphate chain which are based on ($P_2O_6^{2-}$) groups. This suggests that PbO play an intermediate role with breakage of P–O–P bonds and forming PbO_4 tetrahedral units. The addition of less than 15 mol% PbO produces a small effect on water durability because the hydrolysis reaction of covalent P–O–P bonds and/or the hydration reaction occurs at modifier cations of P–O..Li, are predominant linkages in glasses with the lowest PbO contents. Above 15 mol% PbO, the formation of more and more P–O–Pb bonds, increases the cross-link between the phosphate chains and overall, enhance dramatically water durability and increase of T_g.

References
1. M.R. Ahsan, M.G. Mortuza, *J. Phys. Chem. Glasses*. 42 (2001) 1-5.
2. B. Tiwari, A. Dixit, V. Kothiyal, M. Pandey, S.K. Deb, *Barc Newsletter*. 285 (2007) 167-173.
3. I. Abrahams, E. Hadzifejzovic, *Solid State Ionics*. 134 **(**2000) 249–257.
4. A. Bhide, K. Hariharan, *Mater. Chem. Phys*. 105 (2007) 213.
5. R.K.Brow, *J. Non-Cryst. Solids*. 263&264 (2000) 1–28.
6. L. Hu, D. He, H. Chenet al., *Opt Mater*. 63 (2017) 213-220.
7. J. Yu, Y. Gu, Q. Zhang, Z. Luo, A. Lu, *Mater. Lett*. 212 (2018) 25–27.
8. T. Ishiyama, S. Suzuki, J. Nishii, T. Yamashita, H. Kawazoe, T. Omata, *Solid State Ionics*. 262 (2014) 856
9. A.V. Chandrasekhar, A. Radhapathy, B.J. Reddy, *Opt Mater*. 22(3) (2003) 215–220.
10. H. Yung, P.Y. Shih, H.S. Liu, T.S. *Chin, J. Am. Ceram. Soc*. 80 (1997) 2213–2220.
11. R. Saidi, M. Fathi, H. Salimijazi, *J. Alloys Compd*. 727 (2017) 956–962.
12. J.R. Van Wazer, Phosphorus and its Compounds Volume I: Chemistry. Vol. 1. *New York: Interscience Publishers, Inc*. (1958).
13. L.Koudelka, I. Rösslerová, J.Holubová, P.Mošner, L.Montagne, Be.Revel, *J. Non-Cryst. Solids*, 357 (2011) 2816–2821.
15. W. Donald, B.L. Metcalfe, R.N.J. Taylor, *J. Mater. Sci*., 32 (1997) 5851–5887.
16. F.H. ElBatal, M.A. Marzouk, A.M. Abdelghany, *J. Non-Cryst. Solids*, 357 (2011) 1027–1036.
17. H. Es-soufi, L. Bih, B. Manoun, P. Lazor, *J. Non-Cryst. Solids*, 463 (2017) 12–18.
18. L. Montagne, G. Palavit, R. Delaval, *J. Non-Cryst. Solids* 223 (1998) 43–47.
19. H. Takebe, Y. Baba, M. Kuwabara, *J. Non-Cryst. Solids*, 352 (2006) 3088–3094.
20. K. Meyer, *J. Non Cryst. Solids*, 209 (1997) 227–239.

21. P. Pascuta, G. Borodi, N. Jumate, I.Vida-Simiti, D. Viorel, E. Culea, *J. Alloys Compd.*, 504(2) (2010) 479.
22. M. El Hezzat, M. Et-tabirou, L. Montagne, *Phys. Chem. Glasses*, 44(5) (2003) 345-348.
23. M. Abid, M. Elmoudane, M. Et-tabirou, *Phys. Chem. Glasses*, 43(5) (2002) 267-270.
24. H.S. Liu, T.S. Chin, *Phys. Chem. Glasses*, 38(3) (1997) 123-131.
25. U. Selvaraj, K.J. Rao, *J. Non-Cryst. Solids*, 104(2-3) (1988) 300-315.
26. K. El-Egili, H. Doweidar, Y.M. Moustafa, I. Abbas, *Physica B*, 339 (2003) 237–245
27. N. Sajai, M. Et-tabirou, A. Chahine, *Phase Transitions* 89(12) (2016) 1225–1235
28. A. Musinu, G. Paschina, G.Piccaluga, *J. Non-Cryst. Solids*, 177 (1994) 97–102.
29. H. Tichá, J. Schwarz, L. Tichý, *J. Mater. Sci.*, 42 (2007) 215–220.
30. H.S. Liu, T.S. Chin, S.W.Yung, *Mater. Chem. Phys.*, 50 (1997)1–10
31. H.S. Liu, P.Y. Shih, T.S. Chin, *Phys. Chem. Glasses*, 37(6) (1996) 227–235
32. G.L. Saout, F. Fayon, C. Bessada, P. Simon, A. Blion, Y. Vaills, *J. Non-Cryst. Solids*, 293–295 (2001) 657.
33. J. Schwarz, H. Ticha, *Sci Pap Univ Pardubice A*. 9 (2003) 79–88.
34. S.W. Young, P.Y. Shioh, T.S. Chin, *Mater. Chem. Phys.*, 57 (1998) 111–116.
35. H. Tichá, J. Schwarz, L. Tichý, R. Mertens, *J. Optoelectron. Adv. Mater.*, 6(3) (2004) 747–753.
36. B.C. Sales, L.A.Boatner, *J. Non-Cryst. Solids*, 79(1-2) (1986) 83–116.
37. H.S. Liu, T.S.Chin, *Phys. Chem. Glasses*, 38(3) (1997) 123–131.
38. V.V. Kharton, Hand book of solid state electrochemistry: Fundamentals, Materials and their Applications, 1. *WILEY-VCH Verlag GmbH & Co. KGaA, Weinheim*, (2009).
39. R. Lakshmikantha, R. Rajaramakrishna, R.V. Anavekar, N.H. Ayachit, *Mater. Chem. Phys.*, 133 (2012) 249– 252.
40. R. Lakshmikantha, R. Rajaramakrishna, N.H. Ayachitc, R.V. Anavekarb, *Solid State Physics AIP Conf. Proc.*, 1447 (2012) 551–552.
41. M. Abid, A. Shaim, M. Et-tabirou, *Mater. Res. Bull.*, 36 (2001) 2453–2461
42. C. Garrigou- Lagrange, M. Ouchetto, B.Elouadi, *Can. J. Chem.* 63 (1985) 1436–1446.
43. L. Montagne, G. Palavit, G.Mairesse, *Phys. Chem. Glasses*, 37(5) (1996) 206–211.
44. R.K. Brow, D.R. Tallant, S.T. Myers, C.C.Phifer, *J. Non-Cryst. Solids*, 191(1–2) (1995) 45–55.
45. M. El Hezzat, M. Et-tabirou, L. Montagne, E. Bekaert, G. Palavit, A. Mazzah, P. Dhamelincourt, *Mater. Lett.* 58 (2003) 60–66.
46. A. Shaim, M. Et-tabirou, *Phys. Chem. Glasses*, 42 (6) (2001) 381–384.
47. E. Husson, J.M. Bény, C. Proust, R. Benoit, R. Erre, Y. Vaills, K. Belkhader, *J. Non-Cryst. Solids*. 238 (1998) 66–74.
48. F. Fayon, C. Bessada, J.P. Coutures, D. Massiot, *Inorg. Chem.* 38(23) (1999) 5212–5218
49. M. Abid, M. Et-tabirou, M. Hafid, *Mater. Res. Bull.*, 36 (2001) 407–421.
50. C. Dayanand, G. Bhikshamaiah, V. Jaya Tyagaraju, M.Salagram, *J. Mater. Sci.*, 31 (1996) 1945–1967.
51. A. Chahine, M. Et-tabirou, M. Elbenaissi, M. Haddad, J.L.Pascal, *Mater. Chem. Phys.*, 84 (2004) 341–347.
52. J.C. Hurt, C.J. Phillips, *J. Am. Ceram. Sot.*, 53 (1970) 269–273.
53. P. Subbalakshmi, N.Veeraiah, *Indian J. Eng. Mater. Sci.*, 8 (2001) 275-284.
54. N.A. Ghoneima, A.M. Abdelghanyb, S.M. Abo-NafaF, A. MoustafaaKh, M. ElBadry, *J. Molecular Structure*, 1035(13) (2013) 209–217.
55. R. B. Rouse, P. J. Miller, W. M. Risen, *J. Non-Cryst. Solids*, 28 (1978) 193.
56. G. Little Flower, M. Srinivasa Reddy, G. Sahaya Baskaran, N.Veeraiah, *Opti. Mater.* 30 (2007) 357–363.
57. G. Little Flower, G. Sahaya Baskaran, M. Srinivasa Reddy, N.Veeraiah, *Physica B* 393(2007) 61–72.
58. G. Sahaya Baskaran, G. Little Flower, D. Krishna Rao, N.Veeraiah, *J. Alloys Compd.* 431 (2007) 303–312.
59. E. Mansour, G. El-Damrawi, *Physica B*. 405 (2010) 137–2143.
60. G. Sahaya Baskaran, N. Krishna Mohan, V. Venkateswara Rao, D. Krishna Rao, N.Veeraiah, *Eur. Phys. J. Appl. Phys.* 34 (2006) 97–106.
61. B. Lakshmana Rao, Y.N.Ch. Ravi Babu, S.V.G.V.A. Prasad, *J. Non-Cryst. Solids*, 382 (2013) 99–104
62. B. Lakshmana Rao, Y. N. Ch. Ravi Babu, P. Syam prasad, S. V. G. V. A. Prasad, *Spectrosc. Lett.* 48 (2014) 90–95
63. B.C. Bunker, G.W. Arnold, J.A. Wilder, *J. Non-Cryst. Solids*. 64 (1984) 291-316.
64. A. El Hadrami, M. Mesnaoui, M. Maazaz, J.J.Videau, *J. Non-Cryst. Solids*, 331 (2003) 228–239.
65. H. Gao, T. Tan, D. Wang, *J. Controlled Release*. 96 (2004) 29–36.

(2018) ; http://www.jmaterenvironsci.com